

## Research paper

# Grafting of abciximab to a microbubble-based ultrasound contrast agent for targeting to platelets expressing GP IIb/IIIa – Characterization and in vitro testing

A. Della Martina<sup>1</sup>, E. Allémann<sup>\*</sup>, T. Bettinger, P. Bussat, A. Lassus,  
S. Pochon, M. Schneider

*Bracco Research S.A., Plan-les-Ouates/Geneva, Switzerland*

Received 19 February 2007; accepted in revised form 17 July 2007

Available online 1 August 2007

---

**Abstract**

Abciximab-grafted ultrasound sensitive microbubbles were developed for the diagnosis of stroke. The antibody fragment abciximab, which binds to the GP IIb/IIIa and  $\alpha_v\beta_3$  receptors expressed by activated platelets, was chosen because most ischemic strokes are due to arterial thrombi that are mainly composed of platelets. The abciximab antibody fragment was activated by reduction of the disulfide bond for grafting on the microbubbles. The suspension was freeze-dried after the grafting was performed directly on the formed microbubbles. Quantification of the amounts of abciximab present on the surface of the microbubbles was assessed semi-quantitatively by flow cytometry, and quantitatively using radio-labeled abciximab. A protocol for human and rat platelets deposition and fixation was implemented and the expression of the GP IIb/IIIa receptor was validated by immunostaining. The abciximab-grafted microbubbles showed high static and dynamic binding to fixed platelets. Detection by ultrasonography of microbubbles bound on white and red clots gave higher signals compared to SonoVue microbubbles.

© 2007 Elsevier B.V. All rights reserved.

**Keywords:** Targeted microbubbles; Abciximab (ReoPro); Ultrasound contrast agents; Activated platelets; GP IIb/IIIa receptor; Static binding; Dynamic binding; Binding on clots

---

**Abbreviations:** AEC Kit, aminoethyl carbazole staining kit; BAC-Sulfo-NHS, biotinamido hexanoic acid 3-sulfo-*N*-hydroxysuccinimide ester sodium salt; BSA, bovine serum albumin; DMSO, dimethyl sulfoxide; DPPE-MPB, 1,2-dipalmitoyl-*sn*-glycero-3-phosphoethanolamine-*N*-[4-(*p*-maleimido-phenyl)butyramide] sodium salt; DPPG, 1,2-dipalmitoyl-*sn*-glycero-3-[phospho-*rac*-(1-glycerol)] sodium salt; DSPC, 1,2-distearoyl-*sn*-glycero-3-phosphocholine; EDTA, ethylenediaminetetraacetic acid tetrasodium salt dihydrate; Extravidin-HRP, horseradish peroxidase-labeled extravidin; Fab, antigen-binding fragment; Go Anti-Hu FITC, anti-human IgG FITC-labeled goat IgG; GVA, glycerol vinyl alcohol aqueous mounting solution; Hu NonSpe Fab, non-specific human Fab; PBS, phosphate-buffered saline; RtS, normal rat serum; TCEP, tris(2-carboxy-ethyl)-phosphine hydrochloride.

<sup>\*</sup> Corresponding author. Bracco Research S.A., 31 route de la Galaise, CH-1228, Plan-les-Ouates/Geneva, Switzerland. Tel.: +41 22 884 88 62; fax: +41 22 884 88 85.

E-mail address: [eric.allemann@brg.bracco.com](mailto:eric.allemann@brg.bracco.com) (E. Allémann).

<sup>1</sup> Present address: Bioring S.A., ch. d'Etraz 2, P.O. Box 67, CH-1027 Lonay, Switzerland.

## 1. Introduction

Stroke is the third leading cause of death and disabilities in industrialized countries. However, the outcomes of actual treatments can be dramatically improved if accurate diagnosis and treatment are performed early enough. Therefore, molecular imaging with specific blood clot-targeting contrast agents is a subject of great interest. Among the available imaging technologies, ultrasound imaging is a widespread portable technique which makes it particularly valuable for imaging a large variety of organs even if transcranial ultrasound still needs improvements due to the attenuation and the aberrations induced by the skull bone [1].

Good recent reviews have summarized the state of the art in the field of targeted ultrasound contrast agents [2–9]. To

date, the large majority of reported targeted ultrasound contrast agents can be separated in two categories according to the type of targeting moiety used: synthetic peptides and antibodies or antibody fragments. Several publications were recently issued reporting efforts to target ultrasound contrast agents to fibrin [10–14] or the GP IIb/IIIa receptor [15–17].

An important part of the antibody-microbubble conjugates were obtained by using biotin–avidin interactions. Targeting was obtained either through multi-step injections [10,11,18] or pre-complex formation before injection. In the first case, biotinylated specific antibodies were first administered, followed by avidin and finally the biotin-bearing microbubbles. In the second case, the biotin-bearing microbubbles were first incubated with avidin, then with the biotinylated specific antibody before being injected. Antibodies were also grafted directly to the contrast agents either via direct reaction of an amine with an amine-reactive group on the microbubbles [19] or using bioconjugate cross-linkers [12–14].

The present work describes the development of a new perfluorocarbon-filled phospholipids-based ultrasound contrast agent targeted to the GP IIb/IIIa receptor, expressed by activated platelets, using abciximab as the targeting moiety. Abciximab is the antigen-binding fragment (Fab) of the monoclonal chimeric antibody 7E3 and is commercially available to prevent cardiovascular complications during or after coronary interventions. Abciximab was grafted to the 1,2-dipalmitoyl-*sn*-glycero-3-phosphoethanolamine-*N*-[4-(*p*-maleimido-phenyl)butyramide] sodium salt (DPPE-MPB) containing microbubbles via reduction of the disulfide bond linking the constant region of the heavy and light chains of the Fab, a strategy which was reported for grafting of Fab fragments to liposomes [20,21]. The rationale behind the choice of this particular target is the dynamically high concentration of GP IIb/IIIa on activated platelets (about 50,000 to 100,000 per platelet), the latter being the most important cellular component of the arterial thrombi [22].

## 2. Materials and methods

### 2.1. Materials

IODO-GEN Pre-Coated Iodination Tubes, D-Salt Polyacrylamide Desalting Columns, Zeba Spin Columns, and tris(2-carboxyethyl)-phosphine hydrochloride (TCEP) were purchased from Pierce.

Tyrosine · HCl, biotinamido hexanoic acid 3-sulfo-*N*-hydroxysuccinimide ester sodium salt (BAC-SulfoNHS), Tween 20, normal human serum, and horseradish peroxidase-labeled extravidin (Extravidin-HRP) were purchased from Sigma.

Ethylenediaminetetraacetic acid tetrasodium salt dihydrate (EDTA), calcium chloride, *tert*-butanol, palmitic acid, dimethyl sulfoxide (DMSO), hydrogen peroxide,

and bovine serum albumin (BSA) were purchased from Fluka.

Aminoethyl carbazole staining kit (AEC Kit), hematoxylin counterstain reagent, and glycerol vinyl alcohol aqueous mounting solution (GVA) were purchased from Zymed.

1,2-Dipalmitoyl-*sn*-glycero-3-[phospho-*rac*-(1-glycerol)] sodium salt (DPPG) and 1,2-distearoyl-*sn*-glycero-3-phosphocholine (DSPC) were purchased from Genzyme. 1,2-Dipalmitoyl-*sn*-glycero-3-phosphoethanolamine-*N*-[4-(*p*-maleimidophenyl)butyramide] sodium salt (DPPE-MPB) was purchased from Avanti Polar-Lipids.

Normal rat serum (RtS) was purchased from Biomeda. Na<sup>125</sup>I (Iodine-125) was purchased from Amersham. Paraformaldehyde was purchased from Riedel-deHaën. Abciximab (2 mg/mL, ReoPro<sup>®</sup> Injectable solution) was purchased from Eli Lilly. Heparin sodium (25,000 U/mL, Liquemin) was purchased from Roche. Human thrombin was purchased from Calbiochem. Poly(ethylene glycol) Mw=4000 g/mol (PEG 4000) was purchased from Clariant. Non-specific human Fab (Hu NonSpe Fab) was purchased from Bethyl. Anti-human IgG FITC-labeled goat IgG (Go Anti-Hu FITC) was purchased from KPL. Anti-human CD41 (GP IIb/IIIa) biotinylated mouse IgG (P2 clone) was purchased from Immunotech.

Injectable grade sodium chloride (0.9% solution) was purchased from B. Braun. Phosphate-buffered saline (PBS) was prepared from tablets (Fluka) using deionized water and filtered on 0.2 µm membrane filters. Tris · HCl buffers were prepared from Trizma · HCl 1 M (Sigma) using deionized water and filtered on 0.2 µm membrane filters.

Cell Culture Thermanox Plastic coverslips were purchased from Nunc.

#### 2.1.1. Material of living origin

Human whole blood was drawn by authorized personnel from healthy volunteers.

Rat and human blood were collected in heparinized or citrate solution-containing Monovette tubes (Sarstedt).

### 2.2. Special preparations

#### 2.2.1. <sup>125</sup>I Radio-labeling of abciximab

Abciximab was iodinated using IODO-GEN Pre-Coated Iodination Tubes according to the manufacturer's recommendations with no modification. The non-reacted <sup>125</sup>I was removed by gel filtration on a PBS-equilibrated D-salt polyacrylamide desalting column and the fractions containing the protein were pooled.

γ-Counts of <sup>125</sup>I-abciximab solutions were measured for 3 min using a Packard Cobra II Auto-Gamma counter. The specific activity of the radio-labeled abciximab in the pool after gel filtration was 700,000 cpm/µg.

#### 2.2.2. Biotinylation of Fabs

Sufficient amount of the BAC-SulfoNHS solution (10 mg/mL in DMSO) was added to the Fab solution (2 mg/mL for the abciximab or 1 mg/mL for the Hu Non-

Spe Fab, both in PBS-EDTA 2 mM) to reach a molar ratio of BAC-SulfoNHS to Fab of 10 to 1. The reaction was allowed to progress for 30 min at room temperature, in the dark, under mild stirring.

The Fab solution was then purified by centrifugation on a Zeba Spin Column equilibrated with PBS. The Fab concentration of the collected fractions was estimated from the absorbance at 280 nm using a Uvikon 933 Double Beam UV/VIS Spectrophotometer. Usually, the first fraction contained more than 85% of the initial Fab amount and was the only fraction kept.

### 2.3. Preparation of biological substrates

#### 2.3.1. Isolation of platelets

Platelet-rich plasma (PRP) was obtained from whole blood, collected on 30 U heparin sodium per mL, after 10 min of centrifugation at 180 rcf in 5 mL polypropylene tubes. A volume of PBS containing 30 U heparin sodium per mL (PBS-Hep), equivalent to that of the collected PRP, was added to the infranatant and was centrifuged for 10 min at 220 rcf. The resulting supernatant platelet-poor plasma (PPP) was collected and pooled with the PRP.

The platelets contained in the pooled PRP and PPP were washed twice by centrifugation for 15 min at 350 rcf for human platelets and at 1000 rcf for rat platelets, removal of the supernatant and resuspension in fresh PBS-Hep by repeated gentle aspiration in and ejection out of a pipette tip. The resuspended platelets were then washed twice in PBS following the same procedure. The human platelets were left at rest for at least 4 hours between each of the washing steps and resuspended as described above from time to time.

#### 2.3.2. Deposition of platelets

The washed platelets were counted using a Coulter Multisizer II and 4 to  $8 \times 10^7$  platelets were loaded in the central wells of 24-wells plates and the suspension volume in each well was adjusted to 400  $\mu$ L with PBS. The plates were centrifuged at 1200 rcf for 7 min. The supernatant was then carefully removed and the deposited platelets were fixed by slow introduction of 500  $\mu$ L of PBS containing 2 wt% paraformaldehyde and incubation at room temperature for 5 min. After incubation, the paraformaldehyde solution was discarded and the platelet-coated wells were rinsed twice by introduction of 1 mL PBS containing 0.05 wt% Tween 20 and shaking over a planar shaker for a few seconds. The rinsing was repeated twice with PBS followed by reintroduction of 1 mL PBS for storage at 4 °C.

Round Thermanox coverslips and glass coverslips 13 mm in diameter were platelet-coated using the same procedure by introducing them in the wells of 24-wells plates at the beginning of the procedure.

#### 2.3.3. Preparation of red and white clots

Red clots were made in 24-wells cell culture plate. Fifty microliters of  $\text{CaCl}_2$  solution 100 mM, 50  $\mu$ L of human

thrombin solution 50 U/mL were added to 400  $\mu$ L of citrated whole blood. The clots were obtained after coagulation and overnight maturation at room temperature. Each clot was then cut with a scalpel to obtain approximately  $2 \times 2 \times 10$  mm pieces.

White clots were made in 3 mL polypropylene test tubes. Hundred microliters of  $\text{CaCl}_2$  solution 100 mM, 150  $\mu$ L of human thrombin solution 10 U/mL were added in 400  $\mu$ L of platelet concentrate diluted with 400  $\mu$ L of saline. The clots were obtained after coagulation and overnight maturation at room temperature. Each clot was then removed from the tubes and cut with a scalpel to obtain approximately  $2 \times 2 \times 10$  mm pieces.

### 2.4. Targeted microbubbles preparation

#### 2.4.1. Formulation of maleimide-functionalized microbubbles

A mixture of 37.5 mol% DSPC, 37.5 mol% DPPG, 20 mol% palmitic acid and 5 mol% DPPE-MPB was loaded in 100 mL round-bottom flasks, and was dissolved together with PEG 4000 in *tert*-butanol. The round-bottom flasks were then frozen and freeze-dried. They were then stoppered and their headspace was replaced by a fluorinated gas.

#### 2.4.2. Microbubbles grafting procedure

Seventy-two milliliters of PBS was added to the round-bottom flask containing the freeze-dried phospholipids. The flask was shaken until complete homogenisation of the resulting microbubbles suspension.

The suspension was centrifuged twice to remove excess phospholipids and dissolved PEG. During centrifugation, the microbubbles form a dense surface layer from which the liquid infranatant is separated and discarded. After the second centrifugation, the supernatant microbubbles were resuspended in a 2 mM solution of EDTA in PBS and transferred to a 50 mL Falcon screw-capped tube.

Tris · HCl and EDTA were added in the Fab (abciximab, 2 mg/mL, or Hu NonSpe Fab, 1 mg/mL) stock solution to reach 50 mM Tris · HCl and 50 mM EDTA. TCEP was added in this solution to reach 1 mM TCEP, and the mixture was left one hour at 37 °C for reduction. The mixture was then spun through a 5 mL Zeba column equilibrated with PBS.

The reduced Fab collected after spinning through the column was then introduced in the microbubbles suspension. The headspace of the tube was gassed, the suspension was mildly agitated for 2.5 h at room temperature, in the dark for Fab grafting.

To remove excess reactants, the suspension was centrifuged twice and each time the infranatant was discarded. After the second centrifugation, the supernatant microbubbles were resuspended and their concentration adjusted to  $4 \times 10^9$  microbubbles/mL in a 10 wt% solution of maltose in PBS and split into 1 mL fractions in 10 mL glass vials. The vials were then freeze-dried overnight. Finally, the vials were stoppered, crimped and gassed again.

### 2.4.3. Microbubbles preparation

The microbubbles were resuspended in the vials using two needles (one for injection and one for gas exhaust). One milliliter of PBS was injected through the rubber stopper and the vial was shaken until the resulting white microbubbles suspension appeared homogeneous. The suspension was then transferred in round-bottom 5 mL glass test tubes and centrifuged. The infranatant was then discarded and the supernatant microbubbles were resuspended in 1 mL fresh PBS (and possibly subsequently further diluted for the needs of specific tests).

## 2.5. Characterization of targeted microbubbles

### 2.5.1. Concentration and size distribution

The concentration and size distribution of the microbubbles suspension were measured using a Coulter Multisizer II equipped with a 30  $\mu\text{m}$  capillary in saline solution.

### 2.5.2. Abciximab quantification on microbubbles by radioactivity

$\gamma$ -Counts of  $^{125}\text{I}$ -abciximab-microbubbles suspensions and/or discarded solutions were measured for 3 min using a Packard Cobra II Auto-Gamma counter.

The amounts of abciximab on the microbubbles were calculated in pmol (using 50,000 g/mol for abciximab) according to the specific activity of the radio-labeled abciximab. For the suspensions obtained after grafting and two washing cycles, the equivalents per vial were calculated dividing the total radioactivity measured by the number of vials into which the suspension was split. After resuspension and one washing of a single vial, the amount of abciximab was calculated according to the radioactivity measured after radiolabeling taking into account of the natural decrease of radioactivity over time and to the number of bubbles and their total surface measured by Coulter Multisizer II.

### 2.5.3. Flow cytometry assays

Two samples of Fab-grafted microbubbles suspension were loaded in two 0.6 mL microtubes and Goat Anti-Hu FITC was added in one of the two suspensions at amounts of ten or more molar equivalents of the estimated amount of proteins present on the microbubbles. The suspensions were vortexed and incubated at room temperature for 30 min under mild agitation. The suspensions underwent two washing cycles by centrifugation and were finally diluted with PBS to the adequate concentration of microbubbles for flow cytometry analysis.

For this test, negative controls were obtained following the same procedure with a non-grafted microbubbles suspension.

For each sample, 100,000 events were collected using a Becton Dickinson FACSort machine equipped with an Argon laser operating at 488 nm. Scatter, forward scatter, and fluorescence emission at 530 nm were analyzed using BD CellQuest Pro software. Settings of the instrument

were adjusted so that less than 1% of the events recorded for unlabeled samples exceeded 10 in fluorescence intensity. Events exceeding that threshold of 10 in fluorescence intensity were considered positive.

### 2.5.4. Static binding on platelets

The platelet-coated wells of a 24-wells plate were filled with the incubation medium, either PBS or 50 vol% serum of the adequate species in PBS, containing  $1 \times 10^8$  microbubbles per well. The plate was then sealed, turned upside down and allowed to settle and incubate for 30 min undisturbed.

After incubation, the suspension of microbubbles was discarded and the platelet-coated wells were rinsed three times. This rinsing consisted of introducing 1 mL of PBS, then shaking over a planar shaker for a few seconds and finally discarding the liquid. The platelet-coated wells were subsequently filled with 1 mL PBS and observed with a Leica Leitz DM IL inverted microscope using a 20 $\times$  magnification objective. Pictures were captured with a 3.2 Mpix digital camera and analyzed using the ImageJ 1.30v software. The bound microbubbles were detected automatically by the software after manual thresholding of the image to the adequate luminosity and the fraction of the surface covered with microbubbles in each field was determined in percent.

### 2.5.5. Dynamic binding on platelets

Dynamic binding tests were performed as a complement to the static binding tests. These assays were carried out using a 24 mm long, 14 mm wide FCS2 parallel-plate flow chamber from Biopetechs Inc. (Butler, PA, USA). The flow chamber was positioned in an inverted Olympus IX 51 microscope equipped with a 40 $\times$  objective. A stage adapter was custom-built to turn the flow chamber upside down. This geometry allowed microbubbles to float and to interact with the target surface during infusion. The target surface was obtained by gluing platelet-coated round coverslips (diameter: 13 mm) to the 40 mm diameter glass coverslips used to close the flow chamber. This construction was mounted in order to leave a gap of approximately 250  $\mu\text{m}$  with the bottom of the chamber (0.5 mm thick gasket).

Microbubbles were diluted to  $5 \times 10^6$  microbubbles per mL in 50 vol% serum of the adequate species, previously filtered on a Sartorius Minisart GF-prefilter, in PBS. The microbubbles suspension was pushed through the flow chamber using an adjustable Auto Syringe® AS50 Infusion Pump, from Baxter (Deerfield, IL, USA), with a 60 mL syringe. The pump flow rate was adjusted to 1 mL/min to obtain a shear rate of approximately  $80 \text{ s}^{-1}$ . After infusion was started, pictures of bound microbubbles were captured with a digital camera every 2 min, for 10 min. After 10 min, five pictures were taken randomly between the middle and the exit-half of the coverslips.

A quantitative analysis of microbubble accumulation was performed by counting the number of microbubbles

Fig. 1. General scheme of the grafting reaction of the TCEP-reduced abciximab onto the DPPE-MPB functionalized microbubbles.



corresponds to a yield of about 50%, with a volume average diameter  $D_v$  of approximately 3.2  $\mu\text{m}$ .

One of the key parameters of the targeted microbubbles is the amount of targeting moiety present on their surface. In order to assess this parameter, several methods were explored.

Radiolabeling of the abciximab was chosen in order to quantify definitively the amount of abciximab grafted on the microbubbles. Moreover, tracking the radioactivity of microbubbles suspensions during the grafting procedure allowed the determination of the grafting reaction yields. The results of abciximab quantification by radioactivity measurements are presented in Table 1.

It can be seen in Table 1 that the grafting yield increases with the molar ratio of abciximab to DPPE-MPB. This is likely due to the higher abciximab concentration in the reaction medium as all reactions were performed using equal volumes and microbubbles concentrations. After resuspension of the freeze-dried microbubbles the yield of abciximab on the microbubbles followed roughly the resuspension yield.

Fig. 2 compares the number of abciximab Fab molecules calculated according to the radioactivity measurements with the mean fluorescence intensity measured by flow cytometry (FACS) after incubation with Go Anti-Hu FITC IgG.

The molar ratio of FITC-labeled antibody to grafted Fab of 10 to 1 or more was chosen after a saturation test. In this test, increasing amounts of FITC-labeled antibody were added to microbubbles suspension samples of equivalent surfaces. This test showed that above 10 to 1 molar ratio, the fluorescence signal obtained was not dependent on the amount of FITC-labeled antibody added to the microbubbles suspension anymore. However, the fluorescence measured in different assays was variable. Thus, in order to be able to compare the different samples assayed separately, an internal standard was used to normalize the results.

The linearity of the amount of abciximab grafted onto the microbubbles with the abciximab to DPPE-MPB molar ratio observed in the tested range ( $R^2 = 0.9986$  for the number of abciximab Fabs per bubble obtained by radioactivity and  $R^2 = 0.9754$  for the FACS MFI) demonstrates the robustness of the overall grafting procedure.

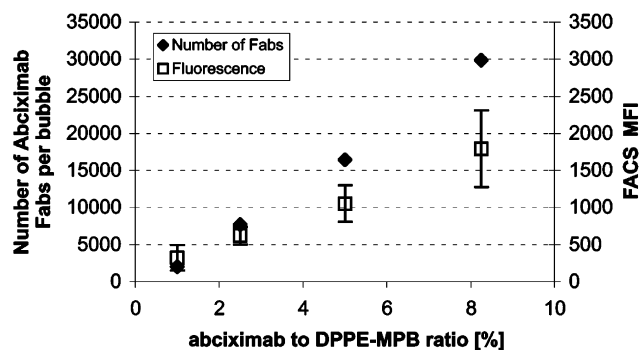


Fig. 2. Number of abciximab Fabs per microbubble calculated using radioactivity measurements and fluorescence measured by flow cytometry after incubation with Go Anti-Hu FITC secondary antibody ( $n = 4$ ), both as a function of initial abciximab to DPPE-MPB molar ratio.

### 3.2. GP IIB/IIIa expression by the platelets and specificity of the binding validation by competition assays

In order to validate the results given by the binding assays on the platelet deposits, it was important to first demonstrate the expression of the GP IIB/IIIa for which the abciximab is specific.

#### 3.2.1. Immuno-histochemistry with human platelet deposits

HRP-conjugated extravidin was used to reveal the binding of biotinylated abciximab, of a biotinylated GP IIB/IIIa specific antibody (positive control), and of a biotinylated Hu NonSpe Fab (negative control) to the human platelet deposits.

The micrographs presented in Fig. 3 clearly show that the biotinylated abciximab gives a positive response even though it seems slightly less intense than the Mo Anti-Hu CD41 IgG. This is likely to result from the divalence of the IgG compared to the monovalence of the Fab giving a higher avidity to the former. The non-specific Fab and the platelets without primary incubation gave little and no response, respectively. Replicates of the presented experiment gave similar results, which indicates that the platelets deposited with the selected method effectively expressed the GP IIB/IIIa receptor.

Table 1  
Radioactivity measurements, related abciximab quantification, and FACS mean fluorescence intensity

Abciximab to DPPE-MPB molar ratio [%]	Introduced for grafting [pmol]	Abciximab quantity equivalents per vial						FACS MFI
		After grafting + 2 washings		After resuspension				
		On microbubbles [pmol]	Yield [%]	On microbubbles [pmol]	Yield [%]	Number of Fabs per microbubble	Number of Fabs per $\mu\text{m}^2$	
1	1104.8	539.3	48.8	201.7	37.4	1970	219	356.09
2.5	2729.5	1377.1	50.5	772.1	56.1	7672	755	627.37
5	5459.0	3076.1	56.3	2006.5	65.2	16408	1415	1242.40
8.25	9257.2	5976.2	64.6	3674.3	61.5	29826	2489	1815.46

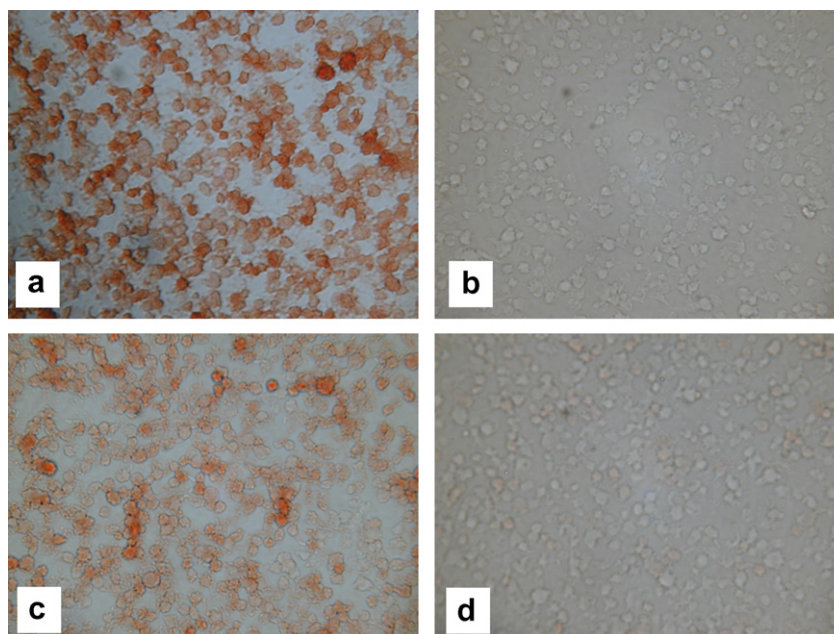


Fig. 3. Micrographs (objective 100 $\times$ ) of immuno-histochemistry assays performed on human platelet deposits. Primary incubation with: (a) biotinylated Mo Anti-Hu CD41 IgG, (b) PBS, (c) biotinylated abciximab, and (d) biotinylated Hu NonSpe Fab. Secondary incubation was with HRP-conjugated extravidin for all conditions.

### 3.2.2. Rat platelet deposits

It is known from the literature that abciximab, the monovalent Fab form of the c7E3 clone, does not bind on rat platelets while the divalent  $F(ab)_2'$  form does [23]. To circumvent this problem, the biotinylated abciximab was incubated with HRP-conjugated extravidin to form a tetraivalent complex. A similar complex was made with the biotinylated Hu NonSpe Fab to serve as negative control in the test. The rat platelet deposits were then tested using the same protocol as that used for human platelets. However, none of these complexes gave a positive staining response.

This could result from the rat platelet deposits not expressing the GP IIb/IIIa receptor. However, immuno-histochemical test performed on human platelets deposited in the same conditions revealed this expression. Moreover, the static and dynamic tests performed on the rat platelet deposits (see sections below) demonstrated the binding of the abciximab-grafted microbubbles while the Hu NonSpe Fab-grafted microbubbles did not show any binding. This suggests that the GP IIb/IIIa receptor is actually expressed by the rat platelets.

From these evidences, it was concluded that the system based on biotinylated Fab associated with extravidin was not able to provide the necessary avidity in the present case. The reasons for this failure should be further investigated.

### 3.3. Static binding on platelets

Static binding tests, on both human and rat platelets, were performed using the batches produced with different

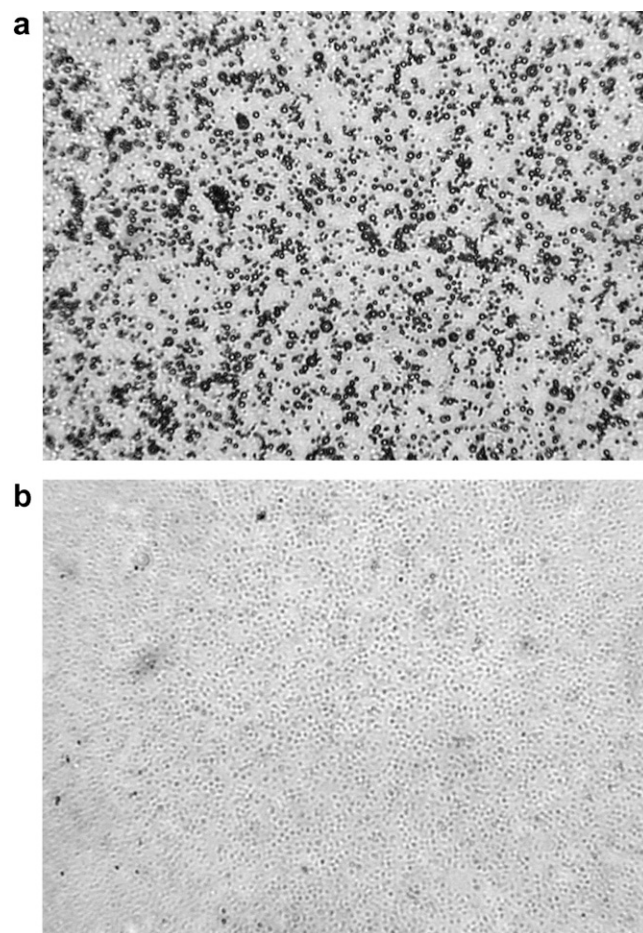


Fig. 4. Example micrographs of static binding assays on human platelets, performed in 50% human serum, of (a) abciximab-grafted, and (b) Hu NonSpe Fab-grafted microbubbles.

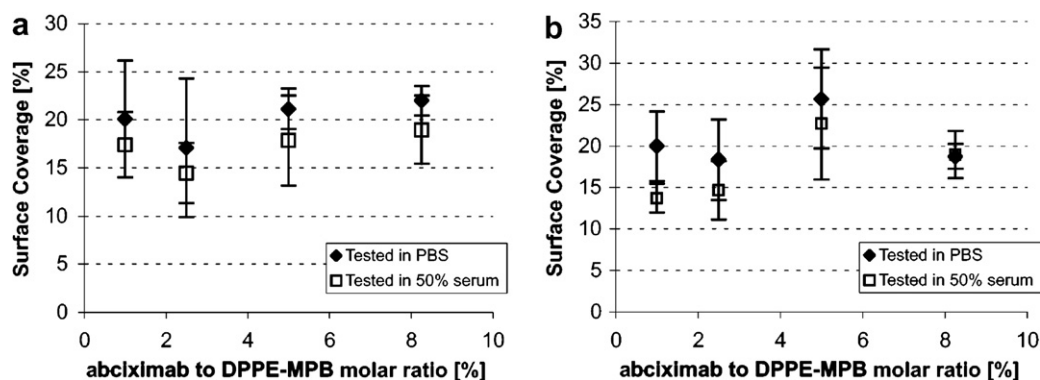


Fig. 5. Results of static binding tests with the samples produced with different initial abciximab to DPPE-MPB molar ratios, on (a) human, and (b) rat platelets.

abciximab to DPPE-MPB ratios. Typical micrographs obtained with microbubbles grafted with abciximab and Hu NonSpe Fab are presented in Fig. 4a and b, respectively. Fig. 5 presents the results from four tests for every different abciximab to DPPE-MPB ratio. Surface coverage on human and on rat platelets is expressed in percent.

The standard deviations' overlap shows that the present test is not sensitive enough to differentiate the samples according to their abciximab to DPPE-MPB molar ratio. Initially, statistical test analyses were performed on results obtained with this test using similar batches produced separately in order to demonstrate the repeatability of the procedure. However, as their significance was overcome by these results, these analyses are not presented here.

On the other hand, abciximab-grafted microbubbles showed a statistically significant difference on both human and rat platelets compared to microbubbles grafted with Hu NonSpe Fab using the same initial Fab to DPPE-MPB molar ratio (5%). The average and the standard deviation of surface coverages based on 8 or more static binding assays for each condition are shown in Fig. 6.

### 3.3.1. Competition between abciximab-grafted microbubbles and free abciximab for binding to human platelet deposits

Competition assays between abciximab-grafted microbubbles and free abciximab were performed on human platelet deposits to determine the binding specificity. This test was based on the observation of the bound bubbles' surface coverage decrease due to the competition of free

abciximab present in the medium for static binding. The concentrations of free abciximab used for this test ranged from 0 to 1000  $\mu\text{g/mL}$ , and the test was performed in human serum 50 vol% in PBS. The results of bound bubbles surface coverage are presented in Fig. 7 as a function of the concentration of free abciximab in the medium.

The curve decrease shows that the binding was due to the interaction between abciximab present at the surface of the microbubbles and the platelets. However, it is interesting to notice that even very high free abciximab concentrations cannot completely hinder the binding of the abciximab-grafted microbubbles in these assay conditions. About 80% of the microbubbles binding only is competed off by the free antibody at concentrations of 100  $\mu\text{g/mL}$  and higher. This concentration corresponds to about 400 $\times$  free antibody excess compared to the approximated content of total grafted abciximab present at the surface of the microbubbles sample used in this test (about 0.25  $\mu\text{g}$  grafted abciximab on  $2 \times 10^8$  microbubbles). This likely results from the multivalency of the abciximab-grafted microbubbles, which provide a much higher avidity to the microbubbles compared to the free abciximab. Repetition of the test showed the good reproducibility of the results.

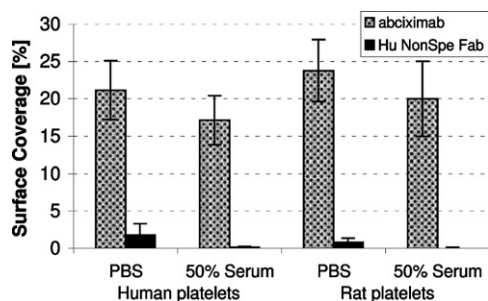


Fig. 6. Differences in static binding results between microbubbles grafted with abciximab and Hu NonSpe Fab on human and rat platelets.

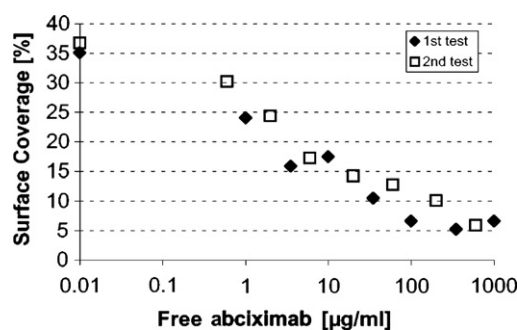


Fig. 7. Competition assays between free abciximab and abciximab-grafted microbubbles. The condition corresponding to absence of free abciximab (0  $\mu\text{g/mL}$ ) in the medium is arbitrarily represented at 0.01  $\mu\text{g/mL}$  on the log scale.



These two tests demonstrate both the suitability of this platelet preparation for testing the binding of the abciximab-grafted microbubbles and the specificity of the abciximab interaction with the platelets deposited with the selected method.

### 3.4. Dynamic binding on platelets

Flow chamber dynamic binding tests on both human and rat platelets were performed using the batches with different fractions of grafted abciximab. The results obtained are presented in Fig. 8.

These results clearly show that, above a certain threshold, the number of bound microbubbles per minute is proportional to the amount of grafted abciximab. This seems to demonstrate the specificity of the binding obtained with grafted abciximab. Below this threshold, the number of bound bubbles is constant. This probably results from the low targeting moieties density on the microbubbles, providing a too limited binding strength to the microbubbles, which were pulled away by the flow in the chamber. Considering the microbubbles grafted using the standard abciximab to DPPE-MPB molar ratio of 5%, the number of bound microbubbles per minute observed in the present test was much higher than that of similar microbubbles with grafted Hu NonSpe Fab. Indeed, the abciximab-grafted microbubbles gave about 4.6 and 1.7 microbubbles bound per minute on human and rat platelets, respectively, while Hu NonSpe Fab grafted samples gave around 0.2 on both substrates. This confirms the superiority of the abciximab-grafted microbubbles over those grafted with Hu NonSpe Fab observed with the static binding test.

### 3.5. Echographic determination of bound bubbles on clots

The results of the quantitative analysis of echographic images obtained at low MI (0.05) with red thrombi incubated with either abciximab or Hu NonSpe Fab microbubbles are shown in Fig. 9. In every condition, the average backscatter intensity is higher for the abciximab microbubbles than for the Hu NonSpe Fab. However, the overlap of abciximab and Hu NonSpe Fab standard deviation bars

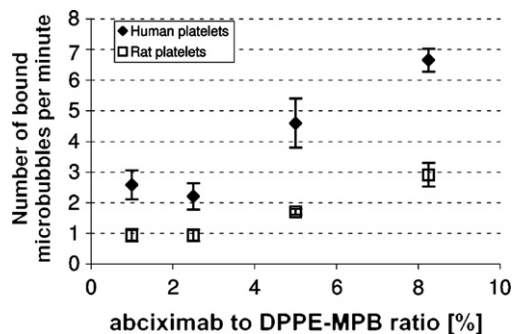


Fig. 8. Results of dynamic binding tests with the samples produced with different initial abciximab to DPPE-MPB molar ratios.

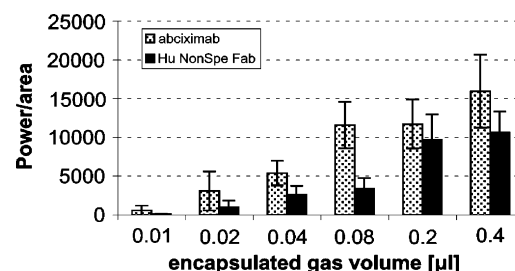


Fig. 9. Results of static binding of abciximab- and Hu NonSpe Fab-grafted microbubbles on red thrombi imaged at low MI (0.05). Results shown are from two series of three thrombi for each condition from which outliers were excluded.

for most the conditions does not allow affirming the superiority of the targeted bubbles over the controls on an individual condition basis.

As observed with the red clots, the average backscatter intensity obtained on white clots with abciximab microbubbles was higher in every condition than those obtained with the Hu NonSpe Fab. These intensities ranged from 100 to 4000 and 100 to 2800 for abciximab- and Hu NonSpe Fab-grafted microbubbles, respectively. However, with white clots also, the standard deviation bars intersected each other.

Measures performed at high MI (0.7) also gave similar results, only with higher power/area absolute values. They ranged from 2500 to 18,000 and 1000 to 15,000 for abciximab- and Hu NonSpe Fab-grafted microbubbles, respectively, on red clots, and from 1000 to 8000 and 1000 to 6000 for abciximab- and Hu NonSpe Fab-grafted microbubbles, respectively, on white clots. With this imaging setting also, the standard deviation bars intersected each other in most conditions.

It is interesting though to compare the results of the binding tests performed on red and white clots. On the two sorts of clots, the binding gives approximately the same results' profile in terms of specificity of the binding of the abciximab-grafted microbubbles compared to the Hu NonSpe Fab-grafted microbubbles (i.e. the ratio of the signals obtained for the two types of microbubbles). However, the absolute value of the signals obtained with the white clots is 3 to 4 times lower than the signal obtained with the red clots. This is surprising as abciximab is specific for receptors expressed by activated platelets. Indeed, the latter are the major component of the white clots, while they represent only a small fraction of the constituents of the red clots, which are mainly made of red blood cells.

It is very difficult to posit an explanation for all these results but it is possible that they arise from the maturation of the clots. Actually, both the red and white clots were prepared one day in advance and left overnight at room temperature. This maturation could allow time for the cross-linking of fibrin to advance and hinder the GP IIb/IIIa receptors initially present at the surface of the clots, reducing the specificity of the binding in both cases. Scanning electron micrographs of clots display essentially fibrin

and platelets are difficultly observed (data not shown). Further work should be done to verify this hypothesis.

#### 4. Conclusion

To the authors' knowledge, this is the first time that an ultrasound contrast agent is combined to a therapeutic agent for targeting purposes. Moreover, it is the first time that a regio-specific reaction is used to graft an antibody or antibody fragment to microbubbles.

The present work demonstrated the potential of abciximab as a grafted moiety to target microbubbles to activated platelets in vitro. To achieve this, methods for human and rat platelets' deposition were developed and the expression of the GP IIb/IIIa receptor by the platelets deposited using these methods was validated for the human platelet deposits. Abciximab-grafted microbubbles showed specific binding to these targets both in static and dynamic conditions, while microbubbles grafted with a similar non-specific Fab did not show significant binding in the same conditions. Moreover, while the static binding test was not sensitive enough to discriminate the different batches of microbubbles with increasing amounts of grafted abciximab, the dynamic binding of such microbubbles was shown to be proportional to the number of abciximab Fabs present at their surface. The binding of the abciximab-grafted microbubbles on red and white clots was high but, the significance of this result suffered from the high binding of the microbubbles grafted with a non-specific Fab on those targets. Further work should be performed to assess this point.

#### Acknowledgements

The fifth framework program of the European Commission is gratefully acknowledged for the financial support of this work through the UMEDS project (Ultrasound Monitoring and Early Diagnostic of Stroke, Grant QL61-CT-2002-01518). P. Emmel is gratefully acknowledged for her help with the immunostaining assays. F. Maisano is acknowledged for fruitful discussions regarding conditions for antibody reduction. Eric V. Dupuis of Bioring SA is gratefully acknowledged for English revision.

#### References

- [1] A. Della Martina, K. Meyer-Wiethe, E. Allémann, G. Seidel, Ultrasound contrast agents for brain perfusion imaging and ischemic stroke therapy, *J. Neuroimaging* 15 (2005) 217–232.
- [2] P.A. Dayton, K.W. Ferrara, Targeted imaging using ultrasound, *J. Magn. Reson. Imaging* 16 (2002) 362–377.
- [3] A.L. Klibanov, Targeted delivery of gas-filled microspheres, contrast agents for ultrasound imaging, *Adv. Drug Deliv. Rev.* 37 (1999) 139–157.
- [4] G.M. Lanza, S.A. Wickline, Targeted ultrasonic contrast agents for molecular imaging and therapy, *Curr. Probl. Cardiol.* 28 (2003) 625–653.
- [5] S.H. Bloch, P.A. Dayton, K.W. Ferrara, Targeted imaging using ultrasound contrast agents. Progress and opportunities for clinical and research applications, *IEEE Eng. Med. Biol. Mag.* 23 (2004) 18–29.
- [6] F.S. Villanueva, W.R. Wagner, M.A. Vannan, J. Narula, Targeted ultrasound imaging using microbubbles, *Cardiol. Clin.* 22 (2004) 283–298.
- [7] H.D. Liang, M.J. Blomley, The role of ultrasound in molecular imaging, *Br. J. Radiol.* 76 (Suppl. 2) (2003) S140–S150.
- [8] A.M. Morawski, G.A. Lanza, S.A. Wickline, Targeted contrast agents for magnetic resonance imaging and ultrasound, *Curr. Opin. Biotechnol.* 16 (2005) 89–92.
- [9] A.L. Klibanov, Ligand-carrying gas-filled microbubbles: ultrasound contrast agents for targeted molecular imaging, *Bioconjug. Chem.* 16 (2005) 9–17.
- [10] G.M. Lanza, K.D. Wallace, M.J. Scott, W.P. Cacheris, D.R. Abendschein, D.H. Christy, A.M. Sharkey, J.G. Miller, P.J. Gaffney, S.A. Wickline, A novel site-targeted ultrasonic contrast agent with broad biomedical application, *Circulation* 94 (1996) 3334–3340.
- [11] G.M. Lanza, K.D. Wallace, S.E. Fischer, D.H. Christy, M.J. Scott, R.L. Trousil, W.P. Cacheris, J.G. Miller, P.J. Gaffney, S.A. Wickline, High-frequency ultrasonic detection of thrombi with a targeted contrast system, *Ultrasound Med. Biol.* 23 (1997) 863–870.
- [12] S.M. Demos, H. Alkan-Onyuskel, B.J. Kane, K. Ramani, A. Nagaraj, R. Greene, M. Klegerman, D.D. McPherson, In vivo targeting of acoustically reflective liposomes for intravascular and transvascular ultrasonic enhancement, *J. Am. Coll. Cardiol.* 33 (1999) 867–875.
- [13] S.M. Demos, H. Onyuskel, J. Gilbert, S.I. Roth, B. Kane, P. Jungblut, J.V. Pinto, D.D. McPherson, M.E. Klegerman, In vitro targeting of antibody-conjugated echogenic liposomes for site-specific ultrasonic image enhancement, *J. Pharm. Sci.* 86 (1997) 167–171.
- [14] A. Hamilton, S.L. Huang, D. Warnick, A. Stein, M. Rabbat, T. Madhav, B. Kane, A. Nagaraj, M. Klegerman, R. McDonald, D. McPherson, Left ventricular thrombus enhancement after intravenous injection of echogenic immunoliposomes: studies in a new experimental model, *Circulation* 105 (2002) 2772–2778.
- [15] E.C. Unger, T.P. McCreery, R.H. Sweitzer, S. DeKang, G.L. Wu, In vitro studies of a new thrombus-specific ultrasound contrast agent, *Am. J. Cardiol.* 81 (1998) 58G–61G.
- [16] I. Tardy, S. Pochon, M. Theraulaz, P. Nanjappan, M. Schneider, In vivo ultrasound imaging of thrombi using a target-specific contrast agent, *Acad. Radiol.* 9 (Suppl. 2) (2002) S294–S296.
- [17] P.A. Schumann, J.P. Christiansen, R.M. Quingley, T.P. McCreery, R.H. Sweitzer, E.C. Unger, J.R. Lindner, T.O. Matsunga, Targeted-microbubble binding selectively to GPIIb IIIa receptors of platelet thrombi, *Invest. Radiol.* 37 (2002) 587–593.
- [18] G.M. Lanza, D.R. Abendschein, C.S. Hall, M.J. Scott, D.E. Scherrer, A. Houseman, J.G. Miller, S.A. Wickline, In vivo molecular imaging of stretch-induced tissue factor in carotid arteries with ligand-targeted nanoparticles, *J. Am. Soc. Echocardiogr.* 13 (2000) 608–614.
- [19] F.S. Villanueva, R.J. Jankowski, S. Klibanov, M.L. Pina, S.M. Alber, S.C. Watkins, G.H. Brandenburger, W.R. Wagner, Microbubbles targeted to intercellular adhesion molecule-1 bind to activated coronary artery endothelial cells, *Circulation* 98 (1998) 1–5.
- [20] S. Shahinian, J.R. Silvius, A novel strategy affords high-yield coupling of antibody Fab' fragments to liposomes, *Biochim. Biophys. Acta* 1239 (1995) 157–167.
- [21] S. Shahinian, J.R. Silvius, High-yield coupling of antibody fab' fragments to liposomes containing maleimide-functionalized lipids, *Methods Enzymol.* 387 (2004) 3–15.
- [22] F.A. Jaffer, R. Weissleder, Seeing within: molecular imaging of the cardiovascular system, *Circ. Res.* 94 (2004) 433–445.
- [23] P.M. Sassoli, E.L. Emmell, S.H. Tam, M. Trikha, Z. Zhou, R.E. Jordan, M.T. Nakada, 7E3 F(ab')<sub>2</sub>, an effective antagonist of rat alphaIIb beta3 and alpha v beta3, blocks in vivo thrombus formation and in vitro angiogenesis, *Thromb. Haemost.* 85 (2001) 896–902.